

Overview of Satellite Thermal Analytical Model

Jih-Run Tsai*

National Space Program Office, Hsin-Chu 300, Taiwan, Republic of China

Thermal analysis is the major engineering work throughout the entire satellite development process, with some crucial stages such as design, test, and ground operations simulation. In the formal design and verification (by test) phases, a general thermal mathematical model for the entire satellite is constructed from a combined conduction and radiation heat transfer equation with environmental heating and cooling as boundary conditions. Some representative numerical schemes with constraints used in satellite thermal analysis, as well as an introduction to the thermal model for the thermal balance test, are presented. However, the general thermal model may be too complicated or inefficient for conceptual design, test monitoring, and ground-operation simulation while developing a satellite. Therefore, simpler governing equations for pure radiation heating and cooling with exact mathematical solutions are developed to fulfill this objective at the expense of analysis accuracy. The linear approximation and exact formulation for solving this simplified problem, as well as the corresponding results shown in graphical form, are also discussed.

Nomenclature

| | |
|-----------------|---|
| A | = cross-sectional area in conduction path or the surface area for radiation exchange, m^2 |
| a | = temperature ratio T_0/T_E |
| C | = thermal capacitance, J/K |
| c | = specific heat, $J/kg \cdot K$ |
| F | = radiation view (shape) factor |
| \mathfrak{F} | = radiation interchange factor |
| G | = conduction conductance, W/K |
| G^r | = radiation conductance, W/K |
| L | = length of the cylinder, m |
| l | = distance between rectangular nodes, m |
| Q | = source term per unit volume, W/m^3 |
| Q_a | = absorbed heat from environment, W |
| Q_i | = internal power dissipation, W |
| \bar{Q} | = heat sources, W |
| q^r | = receiving radiation heat flux on surfaces, W/m^2 |
| R | = radius of the cylinder or sphere, m |
| r | = capacitance to conductance ratio, s |
| T | = temperature, K |
| T_0 | = initial temperature, K |
| t | = time, s |
| V | = node volume, m^3 |
| β | = absorption factor |
| ε | = surface emissivity |
| ε^* | = specified number for convergence |
| ρ | = density, kg/m^3 |
| ρ^d | = surface diffuse reflectivity |
| ρ^s | = surface (first-order) specular reflectivity |
| σ | = Stefan–Boltzmann constant, $5.669 \times 10^{-8} W/m^2 \cdot K^4$ |
| τ | = radiation time constant, s |
| ϕ | = image factor |

Subscripts

| | |
|-----|---|
| E | = equilibrium state |
| i | = specified node numbers (with total node number of N) |
| j | = specified node numbers (with total node number of N) |

w = cold plate or heating shroud

Superscripts

| | |
|-----------|---------------------------------|
| \bar{k} | = time level of the temperature |
| (l) | = iteration level |
| \bar{m} | = time level of the temperature |

Introduction

Thermal analysis is always the major supporting task of satellite or spacecraft thermal engineering work in every development stage, such as design, test, and ground-operation simulation. Thermal analytical techniques have been widely studied and developed in various heat transfer areas^{1–4}; however, the related skills applied in the satellite or spacecraft thermal control are rarely found in the literature.^{5,6} A reliable thermal software package, that is, SINDA⁷ (with a few well-known numerical schemes implemented), has been extensively used to solve the problem for the complex thermal control system in the satellite or spacecraft industry. However, good thermal analytical results should be obtained from not only modeling the thermal system by inserting good enough estimate parameters but also effectively governing the analytical schemes used in the software package for various application purposes. Different analytical models to obtain appropriate solutions, instead of a unique answer from a universal equation, may be chosen for different development stages of the satellite or spacecraft thermal control system. In this paper, a few representative thermal analytical models applied for solving satellite thermal problems are introduced.

A general thermal mathematical model (TMM) with worst hot and cold space environments as boundary conditions used to simulate complex satellite or spacecraft thermal problems in the design phase may obtain, at the expense of time-consuming calculation, acceptable solutions of transient temperatures at hundreds of different locations. However, there may be quite a few uncertain or inaccurate input parameters existing in the TMM, which may affect the analysis accuracy, including thermal contact resistance between contacting parts, unit thermal properties (such as thermal capacitance, thermal conductivity, infrared emissivity, and solar absorptivity), unit power dissipation, etc. Therefore, a thermal balance test is essential to verify the basic thermal design and to assure that the TMM is reliable for the temperature prediction because the input parameters are proved to be valid. Nevertheless, general thermal analytical models are also used for the test analysis and correlation in the test stage.

Simple thermal analytical models instead of application of a general TMM may be required for test monitoring in the test stage and ground-operation simulation before operating the real flying satellite from the ground. This is because some fast estimated solutions are

Received 8 August 2002; revision received 24 February 2003; accepted for publication 22 March 2003. Copyright © 2003 by the American Institute of Aeronautics and Astronautics, Inc. All rights reserved. Copies of this paper may be made for personal or internal use, on condition that the copier pay the \$10.00 per-copy fee to the Copyright Clearance Center, Inc., 222 Rosewood Drive, Danvers, MA 01923; include the code 0022-4650/04 \$10.00 in correspondence with the CCC.

*Senior Researcher and Section Head, Mechanical Engineering Section, 8F, 9 Prosperity First Road, Science-Based Industrial Park. Senior Member AIAA.

needed for quick and straightforward responses and demonstrations at the expense of analysis accuracy during the thermal balance test monitoring and prelaunch flight-operation simulation. These simple analytical formulations are also quite useful in any satellite system interface check and conceptual design for thermal control because only insufficient or immature given inputs are from this complex system in the very beginning and the solutions have to be obtained quickly and updated repeatedly. To not deviate from the reality too far, care should be taken with use of these cheap and fast answers to the problems by checking the assumptions made for the analytical formulations in advance.

General Thermal Analytical Models

The general partial differential equation of combined heat conduction and radiation with source terms⁸ that can construct the satellite TMM is

$$\rho c \frac{\partial T}{\partial t} = \nabla \cdot (k \nabla T) + \nabla \cdot (q^r) + Q \quad (1)$$

Note that Q in Eq. (1) should consist of the internal heat sources from the power dissipation of satellite components and heaters and the external heat sources from the absorbed orbital heating on the boundary surfaces. The boundary surface radiation described in the second term of the right-hand side of Eq. (1) should comprise the radiation exchanges among all radiation surfaces and the space, as well as the absorbed orbital heating from direct solar radiation, Earth infrared emission, and albedo radiation. Therefore, the traditional boundary conditions expressed by normal heat fluxes through the boundary surfaces, adopted by most heat transfer textbooks, will not be shown here. This is because the so-called boundary conditions for the satellite TMM are actually included in the governing equation (1). The initial conditions are always referred to the starting temperatures in different locations; however, the stabilized orbital temperatures will not be affected by the given values of initial temperatures. The general thermal analytical models can be developed and applied for satellite thermal control design and verification by thermal balance test as shown in the next section.

TMM for Thermal Design

Equation (1) can be converted into a system of finite difference equations by constructing finite difference nodes with the help of a Taylor series approximation. Each node is assumed to be isothermal and to have a constant physical property within the node. Then the satellite TMM accepted by the SINDA code is obtained from integrating Eq. (1) over all of the node volumes^{7,9}:

$$C_j \frac{(T_j^{\bar{k}+1} - T_j^{\bar{k}})}{\Delta t} = \sum_{i=1}^N (G_{i,j} + G_{i,j}^r) (T_i^{\bar{m}} - T_j^{\bar{m}}) + \bar{Q}_j$$

$$\bar{k} = 0, 1, 2, 3, \dots, \quad \bar{m} = 0, 1, 2, 3, \dots, \quad j = 1, 2, \dots, N \quad (2)$$

where for rectangular nodes,

$$G_{i,j} = k_{i,j} A_{i,j} / l$$

for cylindrical shell nodes,

$$G_{i,j} = 2\pi k_{i,j} L / \ln(R_j - R_i)$$

and for spherical shell nodes,

$$G_{i,j} = 4\pi k_{i,j} R_i R_j / (R_j - R_i)$$

and where

$$G_{i,j}^r = \sigma A_i \mathfrak{S}_{i,j} (T_i + T_j) (T_i^2 + T_j^2), \quad \mathfrak{S}_{i,j} = \varepsilon_i \beta_{i,j}$$

$$\beta_{i,j} = \varepsilon_j \phi_{i,j} + \sum_{m=1}^N \rho_m^d \phi_{i,m} \beta_{m,j}, \quad \phi_{i,j} = F_{i,j} + \sum_{k=1}^N \rho_k^s F_{i,j,(k)}$$

$$C_j = \rho c V_j, \quad \bar{Q}_j = Q_j V_j$$

There are a few representative numerical methods for various expression of $T^{\bar{m}}$ according to the different time level (superscript \bar{m}) set for the right-hand side of Eq. (2) as

$$T^{\bar{m}} = \begin{cases} T^{\bar{k}}, & \text{explicit} \\ T^{\bar{k}+1}, & \text{implicit} \\ (T^{\bar{k}+1} + T^{\bar{k}})/2, & \text{Crank-Nicolson} \\ (T^{\bar{k}+1} + T^{\bar{k}-1})/2, & \text{Dufort-Frankel} \end{cases} \quad (2a)$$

The initial temperature will be used if the time level of the temperature is set 0 or less than 0. The (modified) Dufort-Frankel method is a three-time-level finite difference scheme, and the other expressions shown in Eq. (2a) are two-time-level representations. Note that the nonlinear temperature terms $(T_i + T_j)(T_i^2 + T_j^2)$ shown in the radiation conductor G^r of Eq. (2) can be assumed as known values in the time level of $\bar{m} - 1$ while the calculation of temperatures in the time level of \bar{m} is performed. This is an easy and fast way to eliminate the nonlinear property of the temperatures for each time step while solving Eq. (2). However, the iterative calculations in each time step will not be completed until the convergence criteria for all node temperatures are satisfied:

$$|T_j^{(l+1)} - T_j^{(l)}|^{\bar{k}} < \varepsilon^*, \quad j = 1, 2, \dots, N \quad (2b)$$

where superscripts (l) and $(l+1)$ represent two successive iteration levels in the time step of \bar{k} and ε^* is a specified small value for the convergence.

Care should be taken when applying the schemes shown in Eq. (2a) because the issue of numerical stability may exist in a marching problem such as Eq. (2). A stable numerical scheme is one for which errors are not permitted to grow in the sequence of the numerical procedure as the calculation proceeds from one marching step to the next. An important parameter r , that is, $C-G$ ratio, is introduced for the discussion of stability:

$$r_j = C_j / \sum_{i=1}^N (G_{i,j} + G_{i,j}^r), \quad j = 1, 2, \dots, N \quad (3)$$

The explicit scheme is conditionally stable because it is stable only when the chosen time step is less than the $C-G$ ratio, that is, $\Delta t < r_j$, whereas the other schemes shown in Eq. (2a) are unconditionally stable. However, the chosen time step Δt for the unconditionally stable schemes should not be so large that any node temperature cannot converge within specified convergence criteria, although these schemes do not have stability issue.

The value of r_j is also important for the thermal analyzer to determine if the node is considered to be diffusion (ordinary node with capacitance), arithmetic (node with negligible capacitance), or boundary (node with huge capacitance). The arithmetic node should be assumed if the value of r_j is very small; otherwise, the converged node temperatures can hardly be obtained within reasonable time of calculation. Some thermal hardware units, such as thermal blanket and passive radiator tape used in the satellite or spacecraft thermal control, are always assumed to be arithmetic nodes in the steady-state calculation because of their negligible weights compared to other components. However, the boundary node (with fixed temperature) should be assumed if the value of r_j is very large. Deep space and propellant are good examples to be considered as boundary nodes in satellite or spacecraft thermal modeling.

Sometimes a satellite or spacecraft TMM is integrated from a few submodels that are built up in parallel by different sources if a complete TMM is very complicated or very large. However, the TMM system integrator should take care of the conduction and radiation interfaces among these submodels in advance to provide all submodel developers with more straightforward interface information. Four cases of interfaces may exist in each submodel as follows. The first case is where there is no conduction and radiation coupling: It is the simplest case because of no thermal interfaces exist in the submodel, and it can be independently developed without interactions

or iterations with other submodels. The second case is where there is conduction coupling only: The submodel cannot be independently developed without information about the interface linear conductors and temperatures. Therefore, these conductors have to be calculated, and the corresponding interface temperatures must be assumed for each submodel development from the beginning. Then the interface temperatures can be updated after the results obtained from submodel integration and analysis by the TMM system integrator. After a few iterations, the conduction interfaces for all submodels can be precisely developed. The third case is where there is radiation coupling only: The submodel cannot be independently developed without information about the interface radiation conductors and temperatures. The gray-body radiation interchanges among all surfaces are very complicated and many interface radiation conductors may be expected. Hence, the TMM system integrator usually establishes simplified representations of radiation interfaces for each submodel developer by totaling all interface radiation exchange factors and creating a mean effective radiation temperature at the expense of accuracy as follows:

$$\mathfrak{S}_{j,\text{total}} = \sum_{i=1}^N \mathfrak{S}_{j,i}, \quad T_{\text{mean}} = \left(\sum_{i=1}^N \mathfrak{S}_{j,i} T_i^4 / \mathfrak{S}_{j,\text{total}} \right)^{1/4} \quad j = 1, 2, \dots, N \quad (4a)$$

Then the total interface radiation conductor for node j of a submodel can be simply expressed as

$$G_{j,\text{total}}^r = \sigma A_j \mathfrak{S}_{j,\text{total}} (T_j + T_{\text{mean}}) (T_j^2 + T_{\text{mean}}^2), \quad j = 1, 2, \dots, N \quad (4b)$$

After all of the submodels are integrated into a complete TMM, the updated interface radiation conductors and temperatures for all submodels can be obtained and iterated.

The last case is where there is both conduction and radiation coupling: This is the most complicated and realistic and combines the preceding two cases. An alternative is to collect all of the incomplete submodels (without thermal interface modeling) and determine all of the interface couplings among submodels by the TMM system integrator.

TMM for Thermal Balance Test

The satellite thermal analytical formulation, that is, Eq. (1), serves not only for predicting satellite temperatures in the orbit but also for the thermal balance test prediction. The former has boundary conditions of orbital heating or cooling from the space, and the latter has boundary conditions of applied heating or cooling from inside of the thermal vacuum chamber. In general, the satellite thermal balance test consists of two major portions, including thermal equilibrium (thermal balance or steady state) and transient heating or cooling phases.

The thermal equilibrium phases of the thermal balance test include hot and cold balance phases. The hot and cold balance phases are used to achieve thermal equilibrium (steady state) in the test article under simulated hot and cold conditions during the flight. The flight units are not duty cycled during the whole test phase so that the temperature stabilization in hot or cold thermal balance is not affected. Similarly, the thermostat-controlled heaters should be disabled in these phases, and their duty-cycle function and performance be checked in the other dedicated phase. In theory, a single set of test conditions will provide enough data for the thermal model correlation. In practice, it is preferable to minimize the amount of extrapolation required from test conditions to worst-case conditions. Thus, a two-point thermal model correlation where both hot and cold conditions are used minimizes the amount of analytical extrapolation to worst-case conditions.

The steady-state equation (2), with no thermal capacitance, will be used to build the TMM for hot and cold balance phases, and the

steady-state temperatures T_E can be obtained from the following equation:

$$\sum_{i=1}^N (G_{i,j} + G_{i,j}^r) (T_i - T_j) + \bar{Q} = 0, \quad j = 1, 2, \dots, N \quad (5)$$

where orbital-averaged heats for hot and cold cases in flight that are simulated by heating sources such as skin heaters or infrared lamps inside the thermal vacuum chamber are applied to the boundary conditions of test article. Note that the maximum- and minimum-averaged values of the power dissipation \bar{Q} are also used for the hot and cold balance phases, respectively.

The conduction conductance G and the radiation conductance G^r assumed in the model will be verified by the test data after the thermal balance test. The correlated predictions should agree within $\pm 3^\circ\text{C}$ of the test data before the correlated thermal model is used to make the final temperature predictions for the various mission phases. If the pretest prediction significantly deviates from the test result, the correlation between them seems meaningless. In such circumstances, errors should be identified from either the thermal mathematical model or the test itself. The design modification, that is, the change of radiator size, must be done after the test if the final temperature predictions for the flight exceed the allowable analytical limits.

The transient heating (warm-up) and cooling (cool-down) phases are to acquire the transient performance data for the test article during a controlled warm up or cool down between hot and cold extremes. To speed heating and cooling and obtain enough data for correlation of unit thermal capacitance within a few hours, all of the environmental heating powers may be turned on for the former case and turned off for the latter case. The transient-state equation (2) will be used to build up the TMM for the transient warm-up or cool-down phase. The maximum and minimum simulated heating powers can be applied on the exterior surfaces of the satellite to be boundary conditions of heating and cooling cases, respectively. Note that the maximum- and minimum-averaged values of the power dissipation \bar{Q} are also used for heating and cooling phases, respectively. Usually, either the warm-up or cool-down phase chosen in the thermal balance test is sufficient for the verification of transient-state performance, and the cool-down phase is preferred to the warm-up phase because the former case can save power.

The agreements between pretest model predictions and test data can guarantee that the assumption of each unit thermal capacitance used in the model is acceptable. In addition, to satisfy the requirement of $\pm 3^\circ\text{C}$ discussed in thermal equilibrium phases, the pretest transient temperature prediction for each unit should agree to its test result without curve crossing or interception between them during testing period. Otherwise, the prediction model for each unit has to be adjusted by modifying the value of the thermal capacitance C assumed in the TMM. Examples of ROCSAT-1 battery and gyroscopic transient cool-down temperatures from thermal balance test and model predictions are compared, as shown in Figs. 1 and 2 respectively.^{10,11}

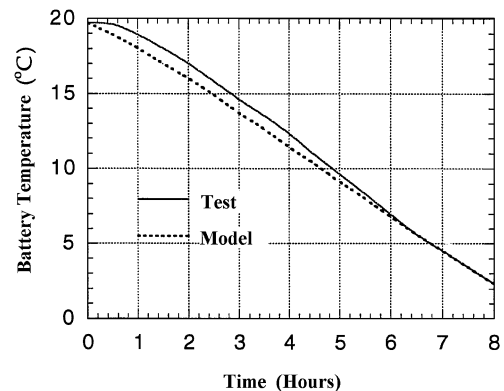


Fig. 1 ROCSAT-1 battery transient cool-down temperature in thermal balance test.

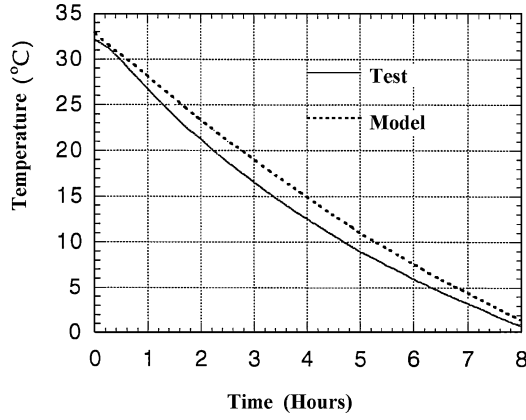


Fig. 2 ROCSAT-1 gyroscopic transient cool-down temperature in thermal balance test.

Simple Thermal Analytical Models

To estimate how far the satellite critical unit temperatures are from their thermal equilibrium states in thermal balance testing, a simple and quick formulation for transient temperatures, instead of the complicated Eq. (2) for a whole satellite, should be developed. In addition, before testing, it is important to estimate how long the test will be conducted from initial to equilibrium states because the appropriate arrangement of test schedule is required for such a complex and time-consuming task. Sometimes unit properties such as emissivity and thermal capacitance can be also determined from measurements of temperature and heat by a radiation cooling or heating test for the unit in a thermal vacuum chamber.⁶ Furthermore, the prelaunch satellite operation simulation for thermal-control personnel training also requires a simple thermal model for some critical units. Thus, the general energy equation (1) is reduced to a simplified case of pure radiation heating or cooling for the isothermal body (with negligible heat conduction) to the environment such as the deep space or a thermal vacuum chamber wall:

$$C \frac{dT}{dt} = \varepsilon A \sigma (T_E^4 - T^4) \quad (6)$$

where $\varepsilon A \sigma T_E^4$ can be obtained from the sum of the body-absorbed radiation energy from the environment Q_a and the internal power dissipation Q_i in steady state, that is,

$$\varepsilon A \sigma T_E^4 = Q_a + Q_i \quad (6a)$$

The constant value of T_E can be obtained if constant (orbit-averaged) Q_a and Q_i are used in the preceding equation, and thus, Eq. (6) can be explicitly solved for the transient temperature T . The case with a nonconstant T_E due to time-varying values of Q_a and Q_i will not be discussed in this paper because it will result in difficulty in solving Eq. (6) without the help from a numerical scheme and, hence, may lose its original advantage of simplicity and convenience.

If the environmental heating is from the adjacent cold plate (or heating shroud) with emissivity ε_w and temperature T_w instead of from the space or thermal vacuum chamber wall, the radiation interchange factor should be introduced between the test-unit radiator and the cold plate. Then, Eq. (6a) for solving T_E can be modified as follows:

$$A \mathfrak{F}_{E,w} \sigma (T_E^4 - T_w^4) = Q_i \quad (6b)$$

If the test-unit radiator is very close to the cold plate (or heating shroud), the radiation interchange factor shown in the preceding equation can be expressed approximately as

$$\mathfrak{F}_{E,w} = \frac{1}{(1/\varepsilon + 1/\varepsilon_w - 1)} \quad (6c)$$

Equations (6b) and (6c) are also useful to estimate the value of T_w for the cold plate applied in the thermal balance test, when T_E has been calculated from Eq. (5) before testing.

Equation (6) can be solved by theoretical analysis, with the result expressed in a compact mathematical formulation; however, Eq. (2) can only be tackled by numerical computation with application to the appropriate thermal software package. Two different solution methods, a linear approximation and an exact formulation to Eq. (6), are described. The former method gives a very simple and explicit solution but may result in more deviations for some cases. However, the latter method, without further restriction, gives an implicit and slightly more complicated solution with a mathematical singularity.

Linear Approximation

When the temperature T is close to the equilibrium temperature T_E , Eq. (6) can be approximately expressed as

$$C \frac{dT}{dt} = 4\varepsilon A \sigma T_E^3 (T_E - T) \quad (7)$$

It is convenient to write Eq. (7) in the form

$$\frac{dT}{dt} = \frac{T_E - T}{\tau} \quad (8)$$

where the radiation time constant τ is defined by

$$\tau = C / 4\varepsilon A \sigma T_E^3 \quad (8a)$$

Note that the time constant is a measure of how rapidly the temperature of the test article will approach its equilibrium value. The solution of Eq. (7) can be obtained as

$$T/T_E = 1 + (a - 1) \exp(-t/\tau), \quad a = T_0/T_E \quad (9)$$

where T_0 is the temperature at $t = 0$, or starting temperature. The temperature approaches the equilibrium temperature T_E , as shown in Fig. 3a when the time gets longer no matter what the value of a is. Note that the value of $a < 1$ represents radiation heating with the limiting case of $a = 0$, whereas $a > 1$ is for radiation cooling with the limiting case of $a = \infty$. The temperatures shown in Fig. 3a have more reliable accuracy for values of a closer to unity (such as the cases between $a = 0.75$ and 1.25) and longer elapsed time due to the assumption of linear approximation made in Eq. (7). The temperature ratios can be also expressed in the form of $1 - \exp(-t/\tau)$ as shown in Fig. 3b, where the temperatures are completely linearized. The temperature difference between the test article (or flight unit) and its equilibrium value usually becomes negligible when it is smaller than the accuracy of temperature measurement, or smaller than any variation in T_E ; the test article can then be considered to reach equilibrium. Thus, the time to reach the equilibrium state t_E can be derived from Eq. (9) and expressed as

$$t_E = \tau \ln[(a - 1)/(E - 1)], \quad E = T_E^*/T_E \quad (9a)$$

where T_E^* is the accepted (approximate) equilibrium temperature in the test or simulation. For the massive satellite component such as the battery with a narrow operating temperature range, that is, value of a close to 1, Eq. (9a) can be easily used to estimate the required equilibrium time once the value of E is set.

Exact Formulation

For lighter but larger components (such as solar array panels, antennas, etc.), the preceding linear approximation may result in solutions with significant deviations and, thus, is not acceptable. Therefore, Eq. (6) must be solved exactly for a more general application and expressed as

$$\frac{dT}{dt} = \frac{T_E^4 - T^4}{4\tau T_E^3} \quad (10)$$

The exact solution of Eq. (10) varies in form depending on whether the initial temperature T_0 is above or below the equilibrium temperature T_E . For the case of radiation heating, the solution can be expressed as

$$(t/\tau) + \text{const} = 2 \left[\tanh^{-1}(T/T_E) + \tanh^{-1}(T_0/T_E) \right] \quad (11)$$

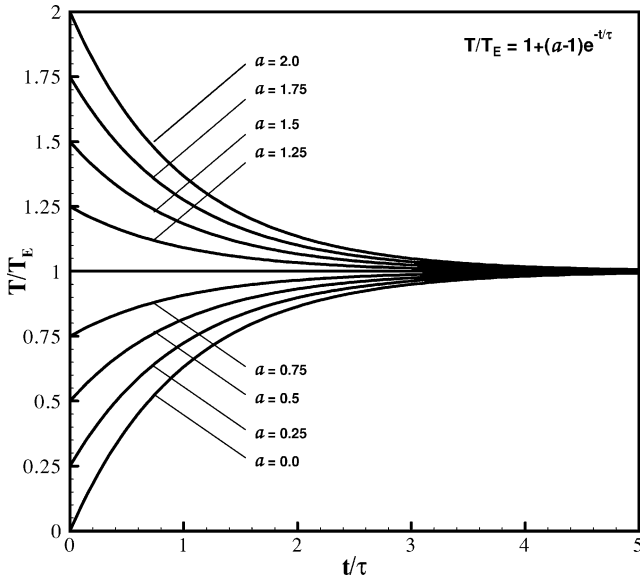


Fig. 3a Linear-approximated temperatures vs t/τ for radiation heating and cooling.

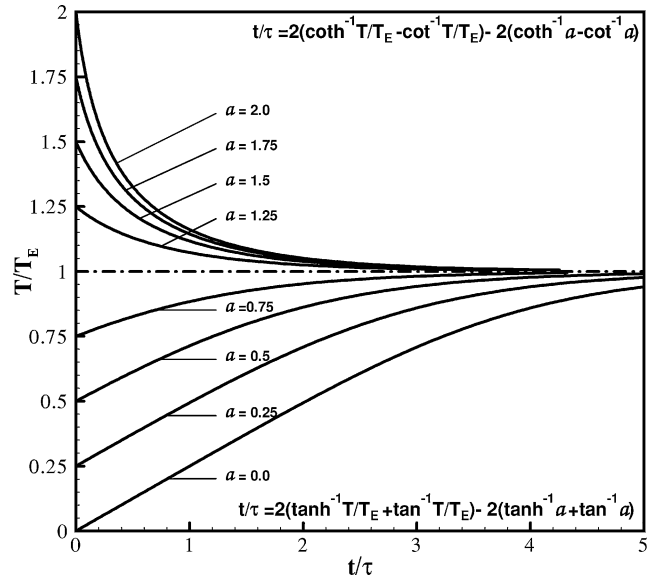


Fig. 4a Temperatures vs t/τ for radiation heating and cooling from the exact formulation.

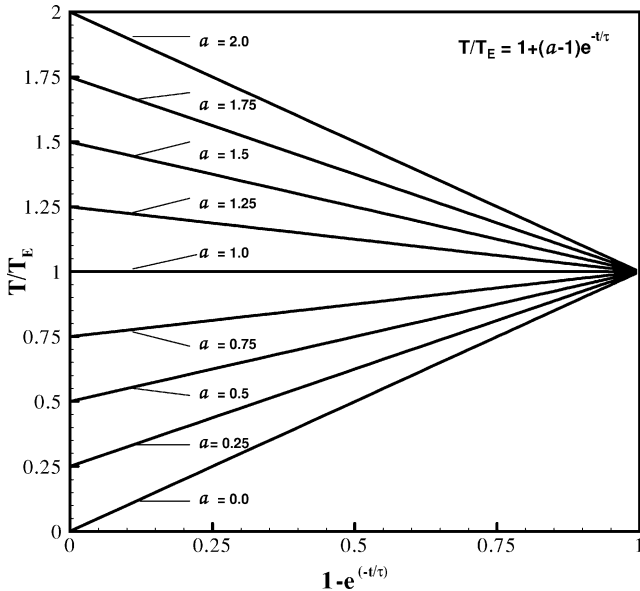


Fig. 3b Linear-approximated temperatures vs $1 - \exp(-t/\tau)$ for radiation heating and cooling.

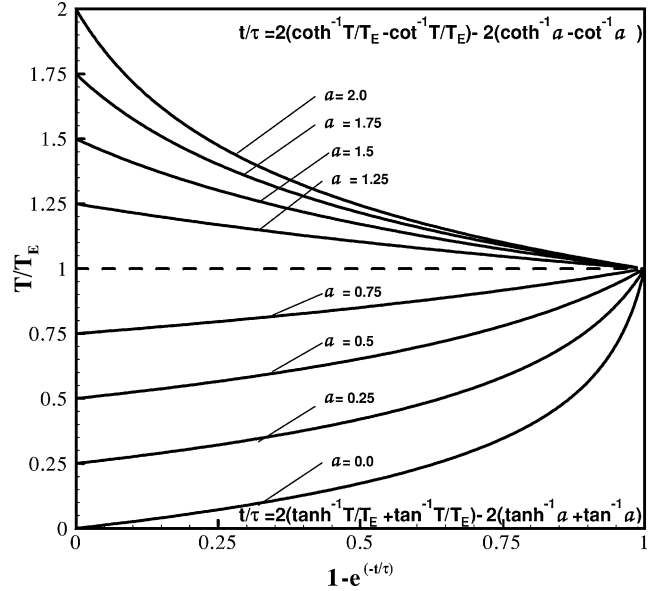


Fig. 4b Temperatures vs $1 - \exp(-t/\tau)$ for radiation heating and cooling from the exact formulation.

where

$$\text{const} = 2(\tanh^{-1} a + \tan^{-1} a), \quad a = T_0/T_E, \quad a < 1 \quad (11a)$$

For the case of radiation cooling, the solution is

$$(t/\tau) + \text{const} = 2[\coth^{-1}(T/T_E) - \cot^{-1}(T/T_E)] \quad (12)$$

where

$$\text{const} = 2(\coth^{-1} a - \cot^{-1} a), \quad a = T_0/T_E, \quad a > 1 \quad (12a)$$

It is not possible to write temperatures as functions of times, although times can be written explicitly as functions of temperatures, as shown in Eqs. (11) and (12), which are plotted in Fig. 4a for various values of a . However, the equilibrium time t_E can be explicitly expressed in Eqs. (11) and (12) when T is substituted for by T_E^* . It is difficult to plot Eqs. (11) and (12) when T_0 approaches T_E because of the singularity occurring at $a = 1$, that is, the case for the temperature always maintained at the equilibrium state. The temperature ratios of Eqs. (11) and (12) can be also expressed in term of $1 - \exp(-t/\tau)$, as shown in Fig. 4b. Sometimes Fig. 4b rather than

Fig. 4a is used if the temperature ratio demonstrated over a whole spectrum of t/τ from 0 to infinity is preferred. Note that the data shown in Fig. 4b have been compressed exponentially when the time is increased. It can be easily found that the temperature approaches the state of equilibrium when the elapsed time is longer than a few times the characteristic time constant τ . Comparing Figs. 4a and 4b with Figs. 3a and 3b, we find the curves with values of a close to 1, that is, $a = 0.75$ and 1.25 , show almost identical transient temperature ratios. These results can prove the validity of the linear approximation applied in the aforementioned cases, and a battery in a satellite with small temperature variations because of its large thermal capacitance before reaching the equilibrium is the best example. However, the results from the exact formulation show that the linear approximation may cause large deviations for the values of a far from unity. The deployed solar array of a satellite with a small thermal capacitance shows large temperature variations, that is, values of a away from 1, before reaching equilibrium in orbit. The cases of $a = 2$ and 0.5 in Figs. 4a and 4b are good examples of solar array radiation cooling when it enters eclipse and heating when it leaves the eclipse in the orbit, respectively.

Conclusions

General, simple thermal analytical models that form the basis of thermal analysis to solve satellite thermal control problems in various development stages have been discussed in detail. The general thermal mathematical model is usually applied in the formal thermal design and test phases, whereas the simple thermal analytical model is frequently used in informal requests for system and test engineering tasks. Both models are equally important to the thermal control problems because the former can lead to complete and quite accurate solutions and the latter is a powerful tool to get quick estimates for the overall system. The fundamental mathematical and numerical background and concepts were briefly introduced for these analytical formulations to confirm assumptions and limitations made for thermal control engineering applications. Experience in satellite thermal control provides the theoretical area of combined conduction and radiation heat transfer with fruitful material for application. A broader bridge has been built between the two sides of academic study in heat transfer and space-engineering application in thermal control.

References

- ¹Smith, G. D., "Parabolic Equations," *Numerical Solution of Partial Differential Equations—Finite Difference Methods*, 2nd ed., Clarendon, Oxford, 1978, pp. 11–74.
- ²Patankar, S. V., "Discretization Methods," *Numerical Heat Transfer and Fluid Flow*, 1st ed., Hemisphere, Washington, DC, 1980, pp. 25–40.
- ³Anderson, D. A., Tannehill, J. C., and Pletcher, R. H., "Basics of Finite

Difference Methods," *Computational Fluid Mechanics and Heat Transfer*, 1st ed., Hemisphere, Washington, DC, 1984, pp. 39–86.

⁴Shih, T. M., "Numerical Methods Used in Heat Transfer (I)," *Numerical Heat Transfer*, 1st ed., Hemisphere, Washington, DC, 1984, pp. 3–42.

⁵Gilmore, D. G., and Collins, R. L., "Thermal Design Analysis," *Satellite Thermal Control Handbook*, edited by D. G. Gilmore, The Aerospace Corp. Press, El Segundo, CA, 1994, pp. 5-1–5-85.

⁶Karam, R. D., "Satellite Thermal Analysis," *Satellite Thermal Control for Systems Engineers*, Progress in Astronautics and Aeronautics, AIAA, Reston, VA, 1998, pp. 91–145.

⁷"SINDA (System Improved Numerical Differencing Analyzer)/G User's Guide," Ver. 1.9, Network Analysis Associates, Tempe, AZ, 1997.

⁸Modest, M. F., "Radiation Combined with Conduction and Convection," *Radiative Heat Transfer*, 1st ed., McGraw-Hill, New York, 1993, pp. 703–758.

⁹Kang, C. S., Huang, J. D., Tsai, J. R., and Ting, L. H., "Satellite Thermal Modeling Techniques and Computation Tools," *40th Conference on Aeronautics and Astronautics*, Aeronautical and Astronautical Society of the Republic of China, Taipei, 1998, pp. 253–260.

¹⁰Tsai, J. R., "ROCSAT-1 Spacecraft Thermal Design/Analysis—Thermal Balance Test," *40th Conference on Aeronautics and Astronautics*, Aeronautical and Astronautical Society of the Republic of China, Taipei, 1998, pp. 229–236.

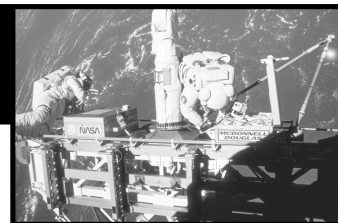
¹¹Tsai, J. R., "Satellite Thermal System Verification—Thermal Balance Test and Thermal Vacuum Test," *Fourth Pacific International Conference on Aerospace Science and Technology (PICAST 4)*, National Cheng-Kung Univ., Tainan, Taiwan, ROC, 2001, pp. 639–645.

I. E. Vas
Associate Editor

Design Methodologies for Space Transportation Systems

Walter E. Hammond

Design Methodologies for Space Transportation Systems is a sequel to the author's earlier text, *Space Transportation: A Systems Approach to Analysis and Design*. Reflecting a wealth of experience by the author, both texts represent the most comprehensive exposition of the existing knowledge and practice in the design and project management of space transportation systems. The text discusses new conceptual changes in the design philosophy away from multistage expendable vehicles to winged, reusable launch vehicles, and presents an overview of the systems engineering and vehicle design process as well as the trade-off analysis. Several chapters are devoted to specific disciplines such as aerodynamics, aerothermal analysis, structures, materials, propulsion, flight mechanics and trajectories, avionics, computers, and control systems. The final chapters deal with human factors, payload, launch and mission operations, and safety. The two texts by the author provide a valuable source of information for the space transportation community of designers, operators, and managers. A CD-ROM containing extensive software programs and tools supports the text.



Contents:

An Overview of the Systems Engineering and Vehicle Design Process ■ The Conceptual Design and Tradeoffs Process ■ Taking a Closer Look at the STS Design Sequence ■ Aerothermodynamics Discipline ■ Thermal Heating and Design ■ Structures and Materials ■ Propulsion Systems ■ Flight Mechanics and Trajectories ■ Avionics and Flight Controls ■ Multidisciplinary Design Optimization ■ Life Support and Human Factors/Ergonomics ■ Payloads and Integration ■ Launch and Mission Operations ■ Related Topics and Programmatic ■ Appendices

AIAA Education Series

2001, 839 pp, Hardcover ■ ISBN 1-56347-472-7

List Price: \$100.95 ■ AIAA Member Price: \$69.95 ■ Source: 945